Site-Augmentation of Empirical Tropospheric Delay Models in GNSS





Daniel Landskron, Gregor Möller, Armin Hofmeister, Johannes Böhm und Robert Weber, Wien

Dieser Beitrag wurde als „reviewed paper" angenommen.

Abstract

Incorrect modeling of tropospheric delays is one of the major error sources in GNSS analysis, as it considerably impairs the accuracy of determined positions. Many GNSS users have no access to real-time information from numerical weather models (NWM), even less to a ray-tracing program capable of directly determining very exact tropospheric path delays. For this reason, empirical troposphere models such as GPT2w (Global Pressure and Temperature 2 wet; Böhm et al., 2015) [1] are of fundamental importance in GNSS analysis. Unfortunately, the accuracy of these empirical models is far worse than that of real-time data, mainly because there is no possibility of capturing short term weather variations, which do not follow seasonal trends. However, in situ meteorological data can be used to significantly improve these empirical models. As is common practice in GNSS analysis, in situ pressure allows very accurate determination of the zenith hydrostatic path delay. In this paper, a new model is proposed revealing new possibilities of improving the zenith wet path delay, which constitutes the main element of uncertainty in troposphere modeling, by additional knowledge of temperature T and water vapor pressure e. Comparison with IGS products or ray-tracing proves the ability of this model to improve empirical zenith wet delays considerably by up to 30%.

Keywords: GNSS, troposphere delay, zenith wet delay, VMF1, GPT2w

Kurzfassung

Die inkorrekte Modellierung troposphärischer Laufzeitverzögerungen ist eine der Hauptfehlerquellen in der GNSS-Auswertung, da sie die Genauigkeit der Positionsbestimmung signifikant beeinträchtigt. Viele GNSS-Nutzer haben keinen Zugriff auf numerische Wettermodelle (NWM) oder gar auf Raytracing-Programme, mit welchen sich die troposphärischen Laufzeitverzögerungen der Signale sehr genau aus den NWM berechnen ließen. Aus diesem Grund kommt empirischen Troposphärenmodellen wie beispielsweise GPT2w (Global Pressure and Temperature 2 wet; Böhm et al., 2015) [1] in GNSS eine besondere Bedeutung zu. Leider ist deren Genauigkeit nicht mit jener von Echtzeitmodellen vergleichbar, was vor allem daran liegt, dass empirische Modelle kurzfristige Wettervariationen nicht erfassen können. Allerdings kann die Genauigkeit empirischer Modelle durch Hinzunahme meteorologischer Messungen an der Station deutlich gesteigert werden; die hydrostatische Zenitlaufzeitverzögerung kann sehr genau aus lokalen Druckmessungen berechnet werden, was in GNSS-Auswertungen ohnehin übliche Praxis ist. In diesem Artikel wird ein Modell vorgestellt, mit welchem die feuchte Zenitlaufzeitverzögerung, die den Hauptunsicherheitsfaktor in der Troposphärenmodellierung darstellt, durch lokale Messungen von Temperatur und Wasserdampfdruck wesentlich genauer bestimmt werden kann als es durch rein empirische Methoden möglich ist. Vergleiche mit hochgenauen IGS-Produkten und Raytracing zeigen schließlich, dass mit diesem Modell die Genauigkeit empirischer feuchter Zenitlaufzeitverzögerungen um bis zu 30% erhöht werden kann.

Schlüsselwörter: GNSS, troposphärische Laufzeitverzögerung, feuchte Zenitlaufzeitverzögerung, VMF1, GPT2w

1. Tropospheric path delay modeling

The slant total path delay $\Delta L(el)$ of a signal is modeled by means of multiplying the path delay in zenith direction ΔL^z with a respective mapping factor mf, which is dependent on the elevation angle el of the observation. For that purpose, the path delay is separated into a hydrostatic and a wet part:

$$\Delta L(el) = \Delta L_h^z \cdot mf_h(el) + \Delta L_w^z \cdot mf_w(el) \qquad (1)$$

The zenith hydrostatic delay ΔL_h^z can be determined very accurately by inserting the in situ measured pressure p into the following equation by Saastamoinen (1972) [2], revised by Davis et al. (1985) [3]:

$$\Delta L_h^z = \frac{0.0022768 \cdot p}{1 - 0.00266 \cdot \cos(2\vartheta) - 0.28 \cdot 10^{-6} \cdot h_{ell}} \quad (2)$$

where ϑ is the colatitude (that is, the complementary angle of the latitude) and h_{ell} is the ellipsoidal height. In case no direct measurement is possible, the pressure value at the earth's surface can also be taken from numerical weather models or, accepting further losses in accuracy, from empirical troposphere models.

GPT2w is such an empirical troposphere model (also referred to as a blind model). Based on either a 5°× 5° or a 1°× 1° grid, it provides mean values plus annual and semi-annual amplitudes of (amongst others) pressure p [hPa], temperature T [°C], water vapor pressure e [hPa], temperature lapse rate dT [°C/km], mean temperature weighted with water vapor pressure T_m [K] and water vapor decrease rate λ [hPa/km]. All those quantities were derived in least-squares adjustments from monthly mean pressure level data of ERA-Interim fields from the ECMWF (European Centre for Medium-Range Weather Forecasts) and can be interpolated for any point on Earth. Empirical tropospheric delay model are needed for applications which do not have access to (considerably more accurate) real-time delays such as those from ray-tracing or VMF1. This may be either due to lacking internet connection or simply because the real-time data is usually only available for specific sites on Earth. Therefore, empirical troposphere models are particularly important for many GNSS applications.

The mapping factors mf_h and mf_w come either from real-time mapping function models such as the Vienna Mapping Functions (VMF1; Böhm et al., 2006) [4] or from empirical models. The most unsteady factor in Eq. (1) is the zenith wet delay ΔL_w^z, because surface measurements of water vapor pressure e alone are only partly representative for the water vapor distribution above the site. Apart from that, ΔL_w^z is highly variable both temporally and spatially and therefore it is very precarious to provide it empirically. As a consequence, empirical zenith wet delays are of very limited accuracy. Nevertheless, a generally used method for calculating them is by applying the formula of Askne and Nordius (1987) [5]:

$$\Delta L_w^z = 10^{-6} \cdot \left(16.5203 + \frac{377600}{T_m}\right) \cdot \frac{R_d}{\frac{\lambda+1}{g_m}} \cdot e \quad (3)$$

where R_d is the specific gas constant for dry constituents which equals 287.0464 $\left[\frac{J}{K \cdot kg}\right]$ and g_m is the mean gravity which equals 9.80665 $\left[\frac{m}{s^2}\right]$.

Here, the input variables water vapor pressure e, mean temperature T_m and water vapor decrease rate λ all come from GPT2w.

2. Site-augmentation of GPT2w

As described in this paper, the performance of GPT2w can be augmented by incorporating in-situ measurements of meteorological quantities such as temperature T, pressure p and water vapor pressure e. Although still remaining only an approximation of the real delay, this site-augmented approach enables a significant improvement in accuracy (in the following, this model is referred to as SA-GPT2w). Meteorological temperature, pressure and humidity sensors can easily be mounted at a GNSS site. While a thermometer and a barometer can directly measure temperature and pressure, respectively, a hygrometer measures the relative humidity f in [%], which in combination with temperature can be converted to water vapor pressure e by means of the so-called "Magnus formula" (see Kraus, 2004) [6]:

$$e = \frac{f}{100} \cdot 6.1078 \cdot e^{\frac{17.1 \cdot T}{235+T}} \quad (4)$$

(note: the e on the right side of the equation expresses Euler's number.) In terms of simplification, in the following there will be talk of the "measured water vapor pressure e", although the quantity actually measured is the relative humidity f.

2.1 Correlation between the quantities

In order to assess the correlation between the quantities, values for temperature T, water vapor pressure e and ray-traced zenith wet delay ΔL_w^z were taken from NWM and the VMF1 files, respectively, for 14 sites around the globe with a temporal resolution of 4 epochs per day from 2011-2014. Investigation of this huge amount of data revealed clear correlations between T and ΔL_w^z and between e and ΔL_w^z, respectively. The degree of correlation can be described by means of the correlation coefficient; its maximum values are 1 and –1, respectively, which means that there is a full (positive or negative) linear relation between

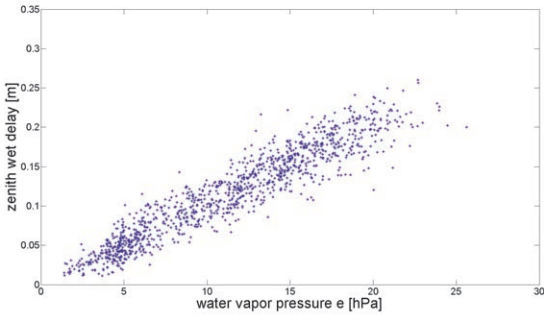

Fig. 1: Correlation between e and ΔL_w^z

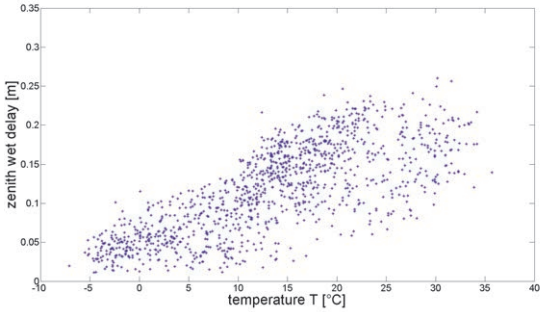

Fig. 2: Correlation between T and ΔL_w^z

two datasets, whereas a correlation coefficient of 0 means that there is no correlation at all. The datasets to be tested here are T vs. ΔL_w^z and e vs. ΔL_w^z. Plotting these to each other yields Figs. 1 and 2; the more the data points approximate a straight line, the higher their correlation coefficient.

The blue points in Fig. 1 represent the relation between water vapor pressure (on the x-axis) and zenith wet delay (on the y-axis) for all 1460 NWM epochs of the year 2013 for IGS station BZRG in Bolzano, Italy. The close-to-line alignment reveals a clear correlation between the two datasets (0.91).

There is also a correlation between temperature and zenith wet delay (Fig. 2), albeit not as distinct as with water vapor pressure. The correlation coefficient for these points of the same data as in Fig. 1 is 0.74.

In a different investigation (Landskron et al., 2015a) [7], correlation coefficients were determined from the NWM data of 14 VLBI (Very Long Baseline Interferometry) stations of all VLBI sessions in the time of 2011 through 2014 (Tab. 1). As this was a VLBI investigation, there was no GNSS data considered. However, the correlations would be virtually the same for GNSS sites.

	Correlation coefficient
between e and ΔL_w^z	0.83
between T and ΔL_w^z	0.61

***Tab. 1:** Correlation between the quantities*

By way of comparison, the correlation coefficient between in situ pressure and the zenith hydrostatic delay ΔL_h^z was determined as 0.995, what means that ΔL_h^z is practically entirely linearly related to p. Nevertheless, also the numbers in Tab. 1 point out distinct correlations between T and e with ΔL_w^z, that allow to infer information about the path delay from those meteorological quantities.

2.2 Concept of SA-GPT2w

The concept of the augmentation is a weighting of differences between the in situ measured meteorological quantities and those from GPT2w. More precisely, three weighting factors M_{zwd}, M_{zwd1} and M_{zwd2} connect differences in temperature and water vapor pressure between in situ measured values and empirical values to the zenith wet delay ΔL_w^z. Eqs. (5) and (6) are the framework of the site-augmented GPT2w.

1. T measured (= SA-GPT2w 1): The universal weighting coefficient M_{zwd} weighs the difference between in situ measured and empirical temperature in order to describe the respective difference in zenith wet delay. This approach is needed, in case the user has the possibility to measure (only) temperature at the site. To do so, Eq. (5) must be applied:

$$\Delta L_w^z = \Delta L_{wGPT2w}^z + M_{zwd} \cdot (T - T_{GPT2\omega}) \quad (5)$$

where ΔL_w^z is the new, augmented zenith wet delay, ΔL_{wGPT2w}^z is the empirical zenith wet delay, determined with the formula of Askne and Nordius (1987) [5] (Eq. (3)), utilizing the input values e, T_m and λ each from GPT2w, and T is the temperature measured at the site.

2. T and e measured (= SA-GPT2w 2): When measuring both temperature T and water vapor pressure e directly at the site, the maximum augmentation of SA-GPT2w can be achieved. Eq. (6) contains two universal weighting coefficients M_{zwd1} and M_{zwd2}, which weigh the differences in temperature and water vapor pressure, respectively, between in situ measured and empirical values in order to infer the respective

difference in zenith wet delay. Eq. (5) is thus extended to

$$\Delta L_w^z = \Delta L_{wGPT2w}^z + M_{zwd1} \cdot (T - T_{GPT2\omega}) + \\ + M_{zwd2} \cdot (e - e_{GPT2w}) \quad (6)$$

where e is the water vapor pressure measured at the site. This describes the wet delays much more precisely than using exclusively temperature as in Eq. (5).

The various M coefficients were determined in least-squares adjustments by replacing in situ T, e and ΔL_w^z with real-time values (Landskron et al., 2015a) [7]; the input values for the measured meteorological data were taken from NWM, and the ΔL_w^z came from ray-tracing through NWM (in fact, from the VMF1 files). At 4 epochs per day from 2009 through 2014, data for 19 VLBI stations, distributed as evenly as possible over the globe, was utilized and inserted into a least-squares adjustment. The resulting M coefficients are listed in Tab. 2.

	M coefficients
M_{zwd}	0.00180 [m/°C]
M_{zwd1}	0.00049 [m/°C]
M_{zwd2}	0.00920 [m/hPa]

Tab. 2: Values for the M coefficients

Apart from that, it was also tested to insert the in situ measured water vapor pressure directly into Eq. (3), without applying any of the augmentation equations (5) and (6). The resulting delays thus turned out to be only slightly worse than those determined with the augmentation.

3. Results

In the following, some ways of estimating the quality of the site-augmented GPT2w are investigated. All of them rely on comparisons with real-time delays which are identified as being highly accurate and close to reality. In all comparisons, mean absolute differences in the delays are determined in order to be able to assess the performance of SA-GPT2w.

3.1 Comparison with delays from GNSS analysis

Utilizing data of a large network of stations that continuously measure signals coming from multiple GNSS satellites simultaneously allows to determine very accurate zenith wet delays. These zenith wet delays can be derived only indirectly, though. In 16 of the 18 IGS analysis centers, special processing techniques are applied capable of combining the measurements of all tracked GNSS satellites at different elevations to compute tropospheric zenith total delays ΔL^z for a certain GNSS station (Jean and Dach, 2016) [8]. The IGS then provides them for a set of IGS stations in two different versions, depending on the latency: "ultra-rapid tropospheric ΔL^z" with a latency of only 2-3 hours and an accuracy of 6 mm, or "final tropospheric ΔL^z" with a latency of maximum 4 weeks and an accuracy of 4 mm (http://igs.org/products) [9]. As the latency of the delays is not at all of interest in this investigation, the final tropospheric products were used. They were eventually downloaded from the website of the Goddard Space Flight Center (GSFC) data center (ftp://cddis.gsfc.nasa.gov/gnss/products). Availability of the related in situ pressure at the stations enables determination of the respective zenith hydrostatic delay ΔL_h^z using the equation by Saastamoinen (Eq. (3)), what in further consequence leads to the zenith wet delay ΔL_w^z by simply subtracting the hydrostatic part from the total delay. These high-precision ΔL_w^z are regarded as the "true" reference values, which are then tried to be approximated with SA-GPT2w.

As mentioned before, availability of high-precision information about pressure at the site is required for the reference values, and temperature T and water vapor pressure e for the SA-GPT2w. Hence, we considered meteorological information from three different sources, each of them described in a separate subsection:

1. p, T and e come from official weather stations operated by a meteorological service, which are located close to the respective IGS stations (see 3.1.1)
2. p, T and e come from a subset of IGS stations that are equipped with in situ meteorological sensors (see 3.1.2)
3. p, T and e come from NWM data of the ECMWF (see 3.2)

3.1.1 Meteorological data from weather stations

Some IGS stations around the world have weather stations in their immediate vicinity which continuously measure the meteorological parameters p, T and e, amongst others. The ZAMG (Zentralanstalt für Meteorologie und Geodynamik) provided us this data. As it was basically recorded in order to feed weather prediction, its quality can be

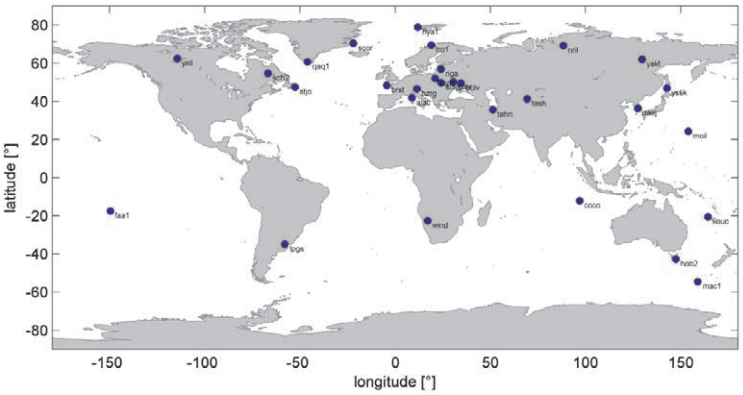

Fig. 3: The 29 IGS stations that each have a close-by weather station in order to estimate the performance of SA-GPT2w for GNSS applications

considered very high. In order to ensure high correlation in the meteorological conditions between the sites of the weather station and the GNSS device, maximum horizontal and vertical distances between them had to be defined; on the one hand, only GNSS stations are used which are less than 10 km away from a weather station. Pressure is fairly steady on the horizontal spatial scale, but in terms of temperature and water vapor pressure distances exceeding this boundary value would be a serious uncertainty factor. On the other hand, there are also differences in altitude between the GNSS stations and the respective weather stations, which may cause similar problems as the horizontal distances, especially for pressure. Here, the limit value is set to 100 meters height difference. Unlike T and e, pressure is vertically extrapolated from the ellipsoidal height of the weather station to the ellipsoidal height of the GNSS antenna in order to ensure highest possible accuracy of the resulting zenith hydrostatic delays ΔL_h^z by assuming a simple pressure lapse rate of 1 hPa per 8 meters.

Considering a temporal resolution of 4 epochs per day for the whole year of 2013, data of 29 relevant IGS - weather station pairs are to be tested. The map in Fig. 3 below shows their locations.

Inserting T and e from the weather stations into Eq. (5) and (6) results in zenith wet delays that are considerably closer to the "real" ΔL_w^z than the empirical ΔL_w^z, as Fig. 4 and Tab. 3 clearly reveal.

	mean. abs. diff. ΔL_w^z [cm]
GPT2w	2.8
SA-GPT2w 1	2.7
SA-GPT2w 2	2.0

Tab. 3: Results of the comparison with high quality zenith wet delays from the IGS averaged over all epochs in 2013. The input parameters T and e come from close-by weather stations.

In terms of SA-GPT2w 1 (using only T) the overall improvement in ΔL_w^z is 5 %, with the majority of stations being brought closer to the "true" delays from the IGS. In contrast, SA-GPT2w 2 (using both T and e) improves the ΔL_w^z by even 29 % on average, yielding an improvement for every single station.

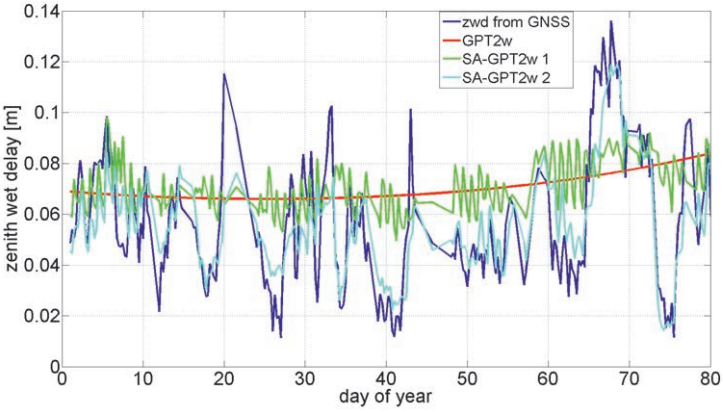

Fig. 4: Comparison of ΔL_w^z from various sources for the IGS station bzrg in Bolzano, Italy during the first quarter of 2013

3.1.2 Meteorological data from IGS in situ sensors

A limited number of IGS stations is equipped in situ with temperature, pressure and humidity sensors capable of measuring meteorological quantities together with the GNSS observations, originally intended for the extraction of precipitable water vapor from the zenith total delay ΔL^z [Hackman and Byram, 2014] [11]. Thus, a perfect spatial and temporal correlation between the meteorological data and the tropospheric delays is ensured.

Unfortunately, it turned out that the quality of this data is fairly poor. Taking the period of 2013 into consideration again, many stations had to be excluded from the analysis beforehand as their meteorological data was simply useless; many stations had entirely wrong measurements, the timestamps of the measurements were not always fully trustworthy and the data format was not even standardized. After exclusion of all affected stations, 26 IGS stations with in situ measured meteorological data remained (Fig. 5).

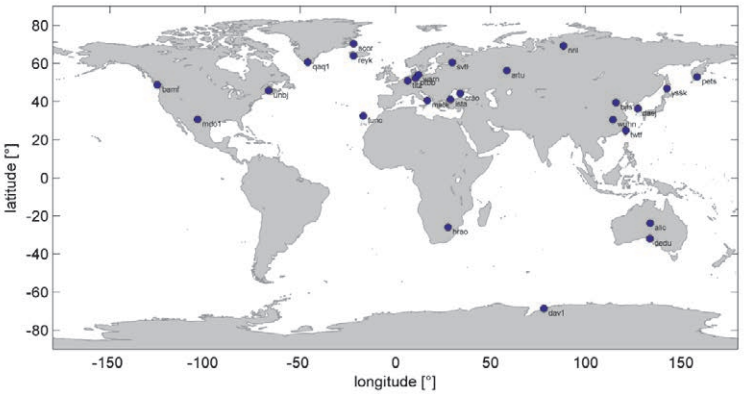

Fig. 5: The 26 selected IGS stations that are equipped with temperature, pressure and humidity sensors in order to estimate the performance of SA-GPT2w for GNSS applications

Fig. 6 shows the augmentation performance for GNSS station artu close to Yekaterinburg Russia during the first quarter of 2013. As this station is located far north (58° 33' 38" N) which results in a generally low water vapor content of the air, measuring T alone yet augments the empirical delay already very well.

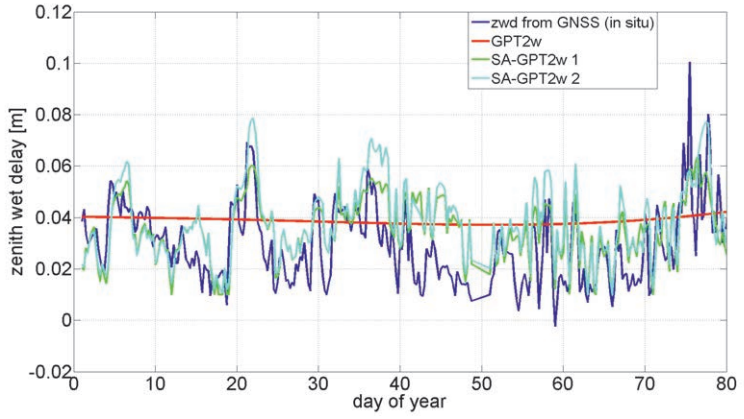

Fig. 6: Comparison of ΔL_w^z from various sources for the IGS station artu in Siberia during the first quarter of 2013

Tab. 4 shows that in situ measurement of T and e, respectively, again yields a significant improvement in augmenting the empirical delays compared to the high precision ones, very similar to the results of the comparison in 3.1.1.

	mean. abs. diff. ΔL_w^z [cm]
GPT2w	2.8
SA-GPT2w 1	2.6
SA-GPT2w 2	2.1

Tab. 4: Results of the comparison with high quality zenith wet delays from the IGS averaged over all epochs in 2013. The input parameters T and e come from meteorological sensors mounted directly at the GNSS sites.

3.2 Meteorological data from NWM of the ECMWF

Eventually, it was tested to which extent SA-GPT2w may improve the results when meteorological data from NWM is utilized for the augmentation. The reference zenith wet delays come from the VMF1-files (that is, from ray-tracing through NWM) instead of the IGS products. Thus, a longer time period and a higher number of stations could be considered, namely 45 GNSS sites at 4 epochs per day from 2011 through 2014 (Fig. 7).

Tab. 5 proves that the augmentation performance is comparable to those where the input data comes from direct measurements. Again, SA-GPT2w 1 improves the results only marginally, whereas SA-GPT2w 2 brings the delays 30 % closer to the real ones. As a conclusion, meteorological input from NWM can be regarded as to be perfectly suited for SA-GPT2w as well. This is of particular importance to users who have access to NWM but no chance of performing ray-tracing through them, which would allow direct

calculation of the delays with significantly higher precision.

	mean. abs. diff. ΔL_w^z [cm]
GPT2w	3.0
SA-GPT2w 1	2.9
SA-GPT2w 2	2.2

Tab. 5: Results of the comparison with ray-traced zenith wet delays. The input parameters for SA-GPT2w, T and e come from NWM interpolated to the very location of the IGS sites.

In addition, the availability of NWM data for the entire network of IGS stations facilitated another investigation; previous analyses revealed that the performance of SA-GPT2w may not yield satisfying results in tropical or generally humid areas [Landskron et al., 2015b; Landskron et al., 2016] [12,13]. NWM data is available for virtually every IGS station situated in close proximity of the equator; thus, a comparison like the one before could be carried out. In fact, data of 13 stations (Fig. 8) close to the equator in the time period of 2011 through 2014 (5868 epochs for each station) was analyzed, which led to the results in Tab. 6.

	mean. abs. diff. ΔL_w^z [cm]
GPT2w	2.8
SA-GPT2w 1	2.9
SA-GPT2w 2	2.5

Tab. 6: Results of the comparison with ray-traced zenith wet delays for near-equatorial GNSS stations. The input parameters T and e come from NWM interpolated to the very locations of the respective IGS site.

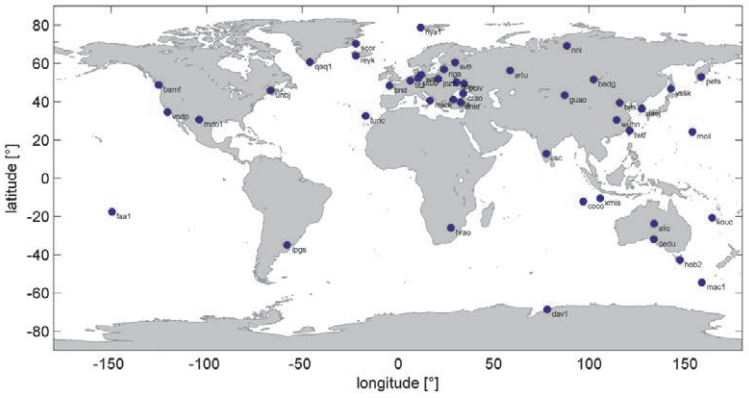

Fig. 7: The 45 IGS stations that were selected for analyzing the potential of meteorological quantities from NWM as input for SA-GPT2w in order to augment the empirical zenith wet delay. These stations are simply those of the two previous GNSS comparisons combined.

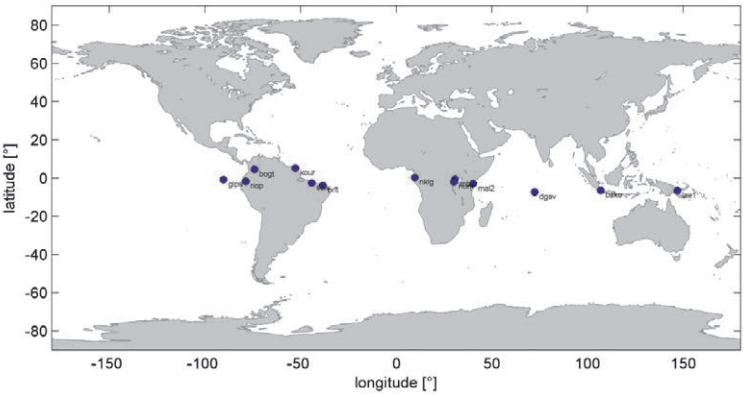

Fig. 8: The 13 near-equatorial IGS stations that were selected for analyzing the potential of meteorological quantities from NWM as input for SA-GPT2w

As expected, the augmentation does not yield a comparable improvement as for the globally distributed stations. The version with using only T for the augmentation even slightly degrades the zenith wet delays and should therefore not be used for sites in humid areas.

4. Conclusions

The conclusions drawn in each of the comparisons from the previous section are very consistent. In general, they can be summarized as follows:

- In situ measurement of temperature T improves the empirical zenith wet delays by approximately 5 % (= SA-GPT2w 1).
- In situ measurement of temperature T and water vapor pressure e improves the empirical zenith wet delays by even up to 30 % (= SA-GPT2w 2).
- In general, best performance of SA-GPT2w is achieved in all areas where the climate is not extraordinarily humid.
- Best performance of SA-GPT2w 1 is achieved at very high latitudes with a very arid climate.

- It was also tested to determine ΔL_w^z by simply inserting the in situ e into Eq. (3) without any further augmentation, which yielded only marginally worse results.
- The model can likewise be applied to VLBI or to other space geodesy analyses.

Taking into account the considerable improvement in accuracy, SA-GPT2w may be of significant importance for all GNSS users, which do not have access to real-time data but have meteorological sensors available in order to make in situ measurements.

References

[1] *Böhm, J., Möller, G., Schindelegger, M., Pain, G., Weber, R. (2015)*: Development of an improved blind model for slant delays in the troposphere (GPT2w). GPS Solutions, 1 (2015), 433-441.

[2] *Saastamoinen, J. (1972)*: Introduction to practical computation of astronomical refraction. Bull. Geod. 106:383-397.

[3] *Davis, J.L., Herring, T.A., Shapiro, I.I., Rogers, A.E.E. and Elgered, G. (1985)*: Geodesy by radio interferometry: Effects of atmospheric modeling errors on estimates of baseline length. Radio Sci., 20(6): 1593-1607.

[4] *Böhm, J., Werl, B., Schuh, H. (2006)*: Troposphere mapping functions for GPS and VLBI from ECMWF operational analysis data. J. Geophys. Res. Vol. 111 B02406, doi:10.1029/2005JB003629.

[5] *Askne, J. and Nordius, H. (1987)*: Estimation of tropospheric delay for microwaves from surface weather data. Radio Science, Volume 22, Issue 3, 379–386.

[6] *Kraus, H. (2004)*: Die Atmosphäre der Erde: eine Einführung in die Meteorologie. Springer Verlag.

[7] *Landskron, D., Hofmeister, A., Böhm, J. (2015a)*: Refined and site-augmented tropospheric delay models for CONT11. EGU General Assembly 2015, Vienna, Austria.

[8] *Jean, Y. and Dach, R. (eds.) (2016)*: International GNSS Service Technical Report 2015 (IGS Annual Report). IGS Central Bureau and University of Bern; Bern Open Publishing DOI: 10.7892/boris.80307.

[9] *Product Description of the International GNSS Service (IGS),* http://igs.org/products. Last access: May 2016.

[10] *GNSS data and products archive of the Crustal Dynamics Data Information Center (CDDIS) at Goddard Space Flight Center (GSFC),* ftp://cddis.gsfc.nasa.gov/gnss/products. Last access: August 2016.

[11] *Hackman, C. and Byram, S. M. (2014)*: Troposphere Working Group Technical Report 2014. In: Jean, J., Dach, R. (eds): IGS Technical Report 2014.

[12] *Landskron, D., Möller, G., Hofmeister, A., Böhm, J., Weber, R. (2015b)*: Refined and Site-Augmented Tropospheric Delay Models for GNSS. Proceedings of the 5th Galileo Science Colloquium, Braunschweig, Deutschland.

[13] *Landskron, D., Möller, G., Hofmeister, A., Böhm, J., Weber, R. (2016)*: Refined and site-augmented tropospheric delay models for GNSS applications. IGS Workshop 2016, Sydney, Australia.

Contacts

Dipl.-Ing. Daniel Landskron, Technische Universität Wien, Department für Geodäsie und Geoinformation, Forschungsgruppe Höhere Geodäsie, Gußhausstraße 27-29, 1040 Vienna, Austria.
Email: daniel.landskron@geo.tuwien.ac.at

Dipl.-Ing. Gregor Möller, Technische Universität Wien, Department für Geodäsie und Geoinformation, Forschungsgruppe Höhere Geodäsie, Gußhausstraße 27-29, 1040 Vienna, Austria.
Email: gregor.möller@geo.tuwien.ac.at

Dipl.-Ing. Armin Hofmeister, Technische Universität Wien, Department für Geodäsie und Geoinformation, Forschungsgruppe Höhere Geodäsie, Gußhausstraße 27-29, 1040 Vienna, Austria.
Email: armin.hofmeister@geo.tuwien.ac.at

Univ.-Prof. Dipl.-Ing. Dr. techn. Johannes Böhm, Technische Universität Wien, Department für Geodäsie und Geoinformation, Forschungsgruppe Höhere Geodäsie, Gußhausstraße 27-29, 1040 Vienna, Austria.
Email: johannes.boehm@geo.tuwien.ac.at

Ao. Univ.-Prof. Dipl.-Ing. Dr. techn. Robert Weber, Technische Universität Wien, Department für Geodäsie und Geoinformation, Forschungsgruppe Höhere Geodäsie, Gußhausstraße 27-29, 1040 Vienna, Austria.
Email: robert.weber@geo.tuwien.ac.at

vgi